CONFERENCE PRE-PRINT

INVESTIGATION OF DOUBLE FREQUENCY FISHBONE IN EAST WITH NEUTRAL BEAM INJECTION

WEI SHEN

Institute of Plasma Physics, Chinese Academy of Sciences Hefei, China

Email: shenwei@ipp.ac.cn

LIOING Xu

Institute of Plasma Physics, Chinese Academy of Sciences Hefei, China

ZHIYONG QIU

Institute of Plasma Physics, Chinese Academy of Sciences Hefei, China

AUTHOR et al.

Abstract

In the EAST experiments with neutral beam injection and at a low electron density, fishbone instabilities characterized by mode numbers m/n = 1/1, 2/2 have been observed. The simultaneous growth of these modes, particularly m/n = 1/1 and m/n = 2/2, results in a decrease in neutron emission at the plasma core. As the electron density continues to decrease, the beta-induced Alfvén eigenmode (BAE) emerges, replacing the m/n = 2/2 fishbone just before a more severe sawtooth crash occurs. Numerical simulations with the global kinetic-magnetohydrodynamic (MHD) code M3D-K show that the m/n = 2/2 high frequency fishbone branch is linearly stable, but nonlinearly grows due to the coupling with the m/n = 1/1 low frequency fishbone branch. The m/n = 2/2 fishbone frequency is almost twice of the m/n = 1/1 fishbone, and both fishbone frequencies chirp down together. The mode frequencies and structures of the simulated fishbones are consistent with the experimental measurements. In addition, a BAE with m/n = 2/2 is observed in the late nonlinear stage of the simulation. Energetic particle nonlinearity is dominant for the m/n = 2/2 fishbone saturation and transition to BAE. In particular, the transition from m/n = 2/2 fishbone to BAE is found to be the consequence of fast ion redistribution due to the fishbone instability.

1. INTRODUCTION

In burning plasmas such as the International Thermonuclear Experimental Reactor (ITER), energetic particle physics is a key issue [1]. Heating of fuel ions by fusion alpha particles is crucial for the self-sustained burning, on the other hand, instabilities excited by energetic particles such as fishbones, could induce energetic particle transport and even losses, and degrade energetic particle confinement. Fishbones were first discovered in the poloidal divertor experiments (PDX), with its name from the shape of Mirnov magnetic signal [2]. There are two early theoretical models developed to explain the fishbone. Chen et al. proposed that the fishbone is driven resonantly by trapped ions via wave particle resonance [3], while Coppi et al. proposed that the fishbone is excited by energetic particles through a positive dissipation process [4].

Hybrid scenario with very flat safety factor q which is around unity in the core region has been recommended for high performance operations in tokamaks. In such scenarios, high-order harmonics with mode number m=n have been observed in many tokamak experiments. In this article, the hybrid kinetic-magnetohydrodynamic (MHD) code M3D-K [5, 6] is applied to analyze the fishbone instabilities with mode numbers m/n=1/1 and 2/2 observed in EAST with neutral beam injection (NBI). It is found that, although the m/n=2/2 high frequency fishbone branch is linearly stable, it can nonlinearly grow to an amplitude around 1/3 of the linearly unstable m/n=1/1 branch fishbone. The transition between the m/n=2/2 high frequency fishbone and the beta-induced Alfvén eigenmode (BAE) is found and analyzed.

2. EXPERIMENTAL OBSERVATIONS

Improving fast ion confinement to enhance plasma performance has been a key research focus for the EAST facility in recent years. The primary source of fast ions in EAST comes from Neutral Beam Injection (NBI). The NBI system is installed at two toroidally separated ports, 112.5 degrees apart, with injection energies spanning the range of 40 to 70 keV, and the total injected power reaching nearly 8 MW. To reduce the loss of fast particles, EAST is usually operated within an edge safety factor range of q_{95} from 3.5 to 4, at a lower plasma electron density $n_e = [2.5 \ 3.5] \times 10^{19} m^{-3}$. In this operational domain, the plasma core tends to exhibit sawtooth-like or fishbone instabilities [32]. Typically, plasmas with a higher level of fast ion confinement, where $q_{min} \sim 1$, are prone to the periodic occurrence of fishbone modes. The presence of these fishbone modes has been observed to contribute to the preservation of the ion temperature transport barrier (Ti-ITB).

In this study, we aim to delve into the enhanced fast ion confinement and explore the formation and evolutionary dynamics of fishbone modes under the conditions of and s \sim 0, with m/n=2/2 fishbone, m and n are toroidal mode number and poloidal mode numbers, respectively. A typical NBI dominant heating discharge #79024, is selected for study in this work. The main parameters are: the power of NBI $P_{NBI} \sim 2MW$ with injected energy about 60keV, the power of low hybrid wave (LHW) $P_{LH} \sim 0.8 MW$, a gradually decrease of n_e from $2.5 \times 10^{19} m^{-3}$ to $2.0 \times 10^{19} m^{-3}$, a moderate plasma current $I_p = 0.45 MA$, a low torodial field $B_{t0} = 1.5 T$, $q_{95}\sim3.6$, a low $\beta_p\sim1.0$ and a relatively high $\beta_N\sim1.5$, the total plasma stored energy $W_{mhd}\sim130kJ$, the thermal energy $W_{thermal} \sim 75 kJ$, the effective charge number in the plasma core Zeff ~ 2.2 and the neutron yield 1.46×10^{14} /s. Figure 1 illustrates that as the plasma density is progressively reduced, two distinct varieties of sawtooth crashes become evident from the core SXR signals. The first variety of sawtooth collapse is marked by a relatively minor amplitude and is accompanied by a fishbone mode driven by fast ions. This particular sawtooth phenomenon is distinguished by two key experimental traits: firstly, the absence of a pronounced thermal plasma-driven precursor m/n=1/1 mode; secondly, the presence of a fishbone mode with an m/n=2/2mode amplitude that rivals the fundamental m/n=1/1 mode. The frequency of the m/n=2/2 mode is double of the m/n=1/1 fishbone mode, and both modes are observed at the same spatial location. The frequency of the fundamental fishbone mode undergoes a decrease from an initial f~20 kHz to f~7 kHz. Collectively, these observations suggest the proximity of $q_{min} \sim 1$, as indicated by the fishbone mode with m/n=2/2.

In contrast, the second type of sawtooth event, depicted in panel (c), is characterized by a more significant collapse amplitude and is associated with an m/n=1/1 fishbone mode, but without a discernible m/n=2/2 fishbone mode. Notably, there is evidence of a thermal plasma-driven m/n=1/1 sawtooth precursor mode (at $f\sim 5$ kHz), which is illustrated in (f) and (g). The present of sawtooth precursor kink mode indicates $q_{min} < 1$. Intriguingly from (g), high-frequency BAEs in the range of $f\sim [60~80]$ kHz emerge prior to the sawtooth collapse, yet they follow the occurrence of the m/n=1/1 fishbone mode in sequence. The mode with a stable frequency of 20 kHz in panel (g) corresponds to the Geodesic Acoustic Mode (GAM) situated at the plasma boundary near $\rho\sim 0.9$.

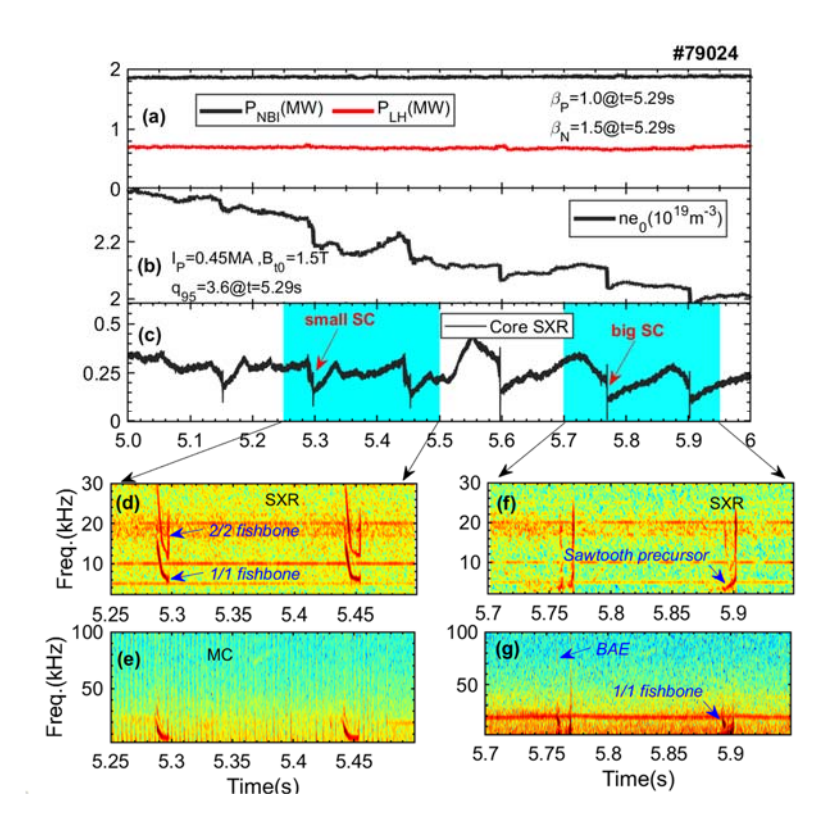


FIG. 1. Observation of m/n=2/2 fishbone and BAE in EAST NBI discharge with a low plasma density.

A zoomed view of SXR and MC spectrograms during two typical sawtooth crashes are depicted in Figure 2. m/n=2/2 fishbone is clearly seen before small sawtooth crash both in SXR and MC spectrograms, as shown in panel (a) and (b). There is no clear sawtooth precursor in small sawtooth crash with m/n=2/2 fishbone. However, there is a precursor, which is believed driven by thermal plasma, presented before big sawtooth crash at $t \sim 5.9$ s. The colormap in panel (d) show that the m/n=1/1 fishbone mode and the m/n=1/1 sawtooth precursor mode possess equivalent strengths, while the intensity of the high-frequency BAEs is a mere one percent of these two. The subtle nature of BAE disturbances means they are only detectable with high-resolution magnetic perturbation measurements. Therefore, for the subsequent spatial structure analysis of perturbation modes, we will concentrate exclusively on the m/n=2/2 fishbone mode.

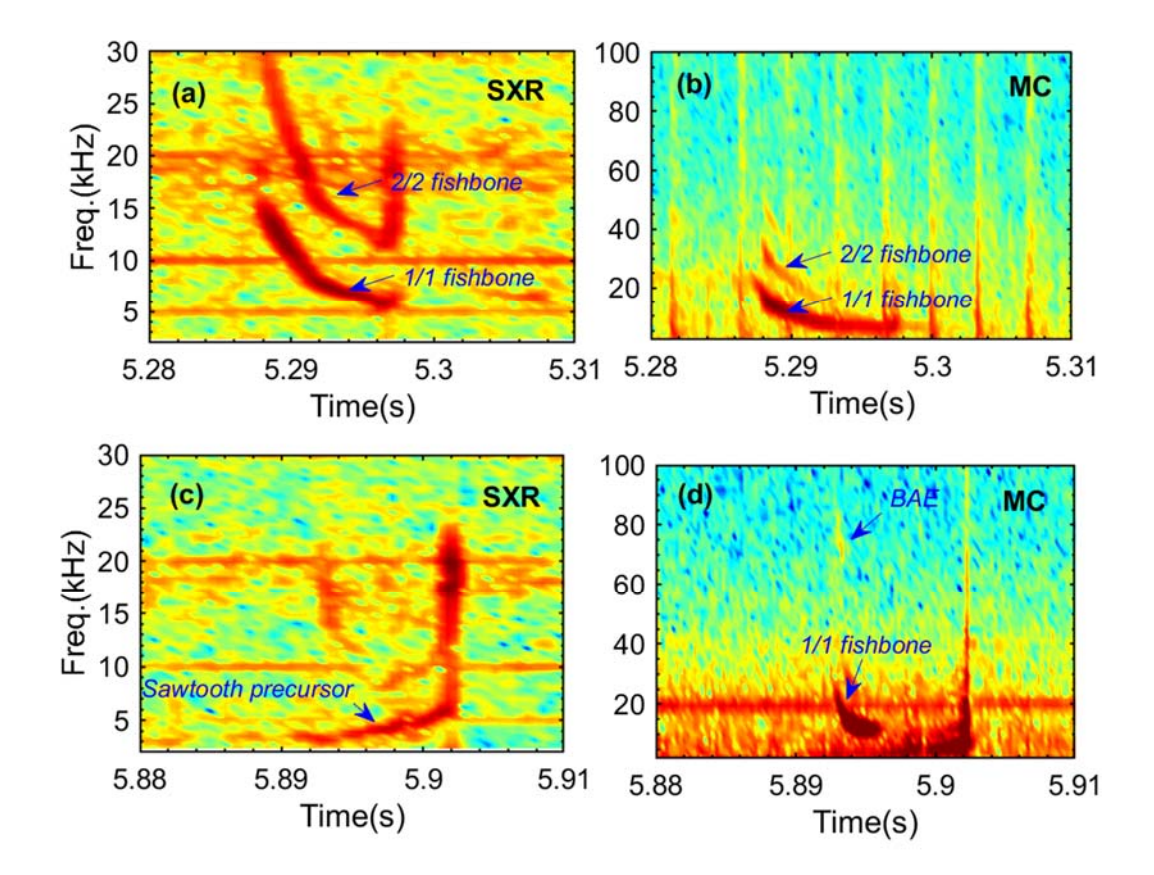


FIG. 2. Zoomed view of SXR and MC spectrogram of m/n=2/2 fishbone and BAE and low frequency sawtooth precursor.

Figure 3 illustrates the temporal progression of the perturbation structure within a fishbone cycle prior to small sawtooth crash, that features an m/n=2/2 fishbone. Singular value decomposition (SVD) method is used to extract the SXR line-integrated perturbations corresponding to different m modes [10], and the colormap in figure 3 represents the SXR line-integrated perturbations with different m modes extracted by SVD method. The dynamics of m/n=1/1 fishbone and m/n=2/2 fishbone are shown in panel (a) and (b), respectively. It is evident that both modes are situated at the same radial location, nestled within the q=1 surface. Two phases have been identified during the fishbone cycle prior to the small sawtooth crash. In phase I, the amplitude of m/n=1/1 mode decreases gradually, and its strength is much stronger than that of m/n=2/2 mode, as shown in (a) and (b) at $t\sim5.2885$ s. In phase II, the amplitude of m/n=1/1 fishbone saturates, while the amplitude of m/n=2/2 fishbone increases. The absence of a clear thermally driven m/n=1/1 kink mode in this type of sawtooth collapse precludes a direct strength comparison between the fishbone mode and the thermally driven kink mode. Interestingly, the heat flux of the m/n=2/2 fishbone changes directions radically from phase I to phase II, as shown in figures 3 (b1) and (b2).

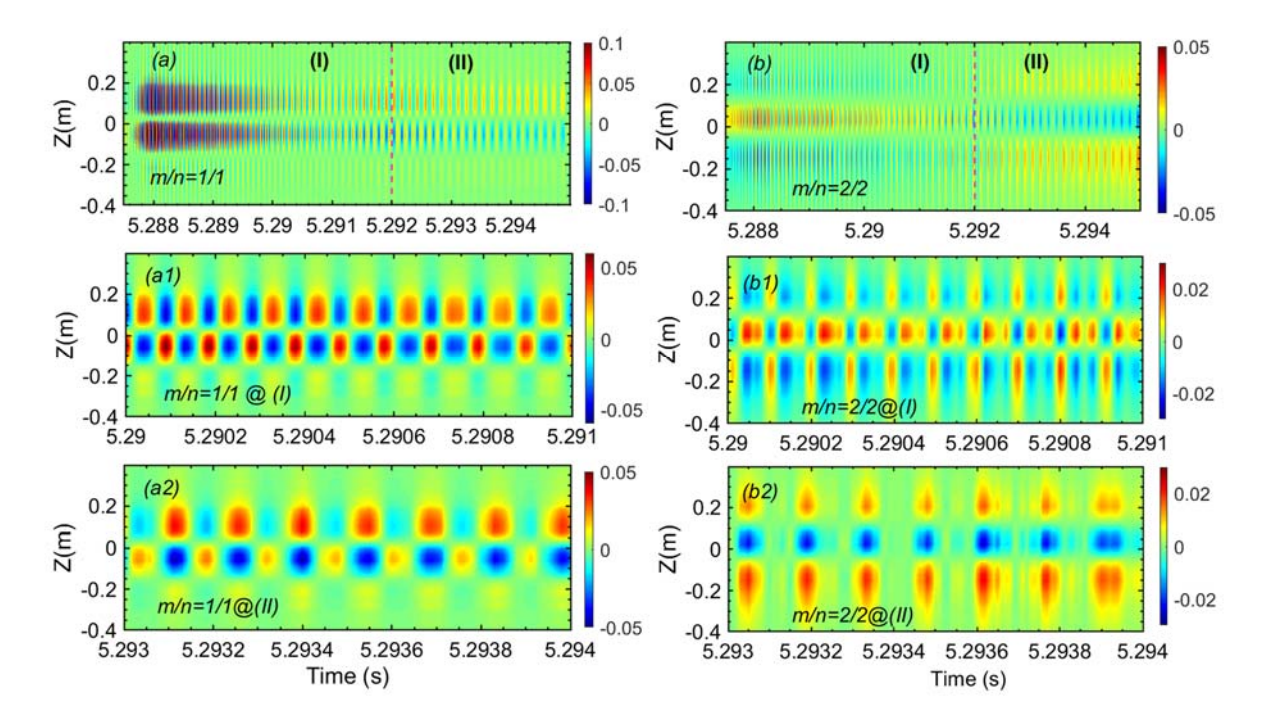


FIG. 3. Fishbone dynamics using multi-channel SXR diagnostic together with singular value decomposition (SVD) method.

As a typical energetic ion driven mode, fishbones including both m/n=1/1 and m/n=2/2 components, could lead to fast particle redistribution in the core region. In EAST, neutron flux evolution is used to monitor the dynamics of energetic ions produced by NBI in the core region. As shown in figure 4, a drop of ~7% is observed during fishbones with m/n=1/1 and m/n=2/2 components. The amplitude of fishbone decreases to a low level at $t \sim 5.295$ s, and the small crash at $t \sim 5.297$ s may be due to the increase of a m/n=2/2 mode, since the crash phase features with up-down symmetry in Z direction.

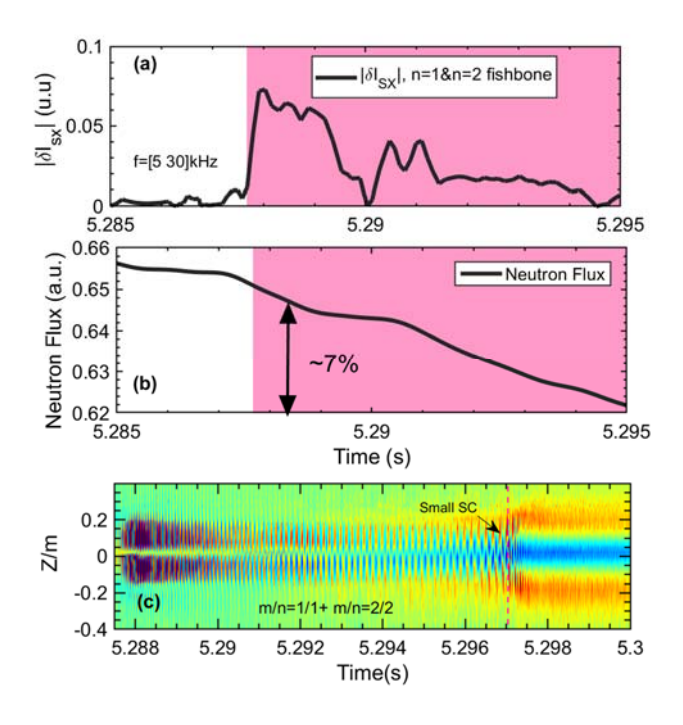


FIG. 4. Neutron flux drop is observed during fishbones with m/n=1/1 and m/n=2/2 components.

3. SIMULATION AND ANALYSIS

The numerical simulations are carried out by applying the global kinetic- MHD code M3D-K, in which the background plasma is described by MHD model while drift kinetic model is used to describe the energetic particles via the particle-in-cell method. The M3D-K code has been widely applied to investigate energetic particle driven instabilities and the interaction between energetic particles and MHD modes. Equilibrium profiles and parameters are chosen at t=5.29 s.

Firstly, linear simulations of the fishbones with m/n=1/1, 2/2 are carried out separately. It is found that the m=n=1 fishbone is unstable, while the m=n=2 fishbone is stable. Secondly, Nonlinear simulations of the fishbone with toroidal mode numbers from n=0 to n=2 show that the m/n=2/2 fishbone grows to maximum mode amplitude around 1/3 of the m/n=1/1 fishbone maximum amplitude, which is shown in figure 5 (b). In addition, as shown in figure 5 (a), it is found that the growth rates of the m/n=1/1 and m/n=2/2 fishbones are $\gamma_{n=1}\tau_A=0.615\%$ and $\gamma_{n=2}\tau_A=1.17\%$ respectively, where $\tau_A=R_0/v_A$ is the Alfvén time. As a result, $\gamma_{n=2}\approx 2\gamma_{n=1}$, which indicates that the m/n=2/2 fishbone is force-driven by the m/n=1/1 fishbone.

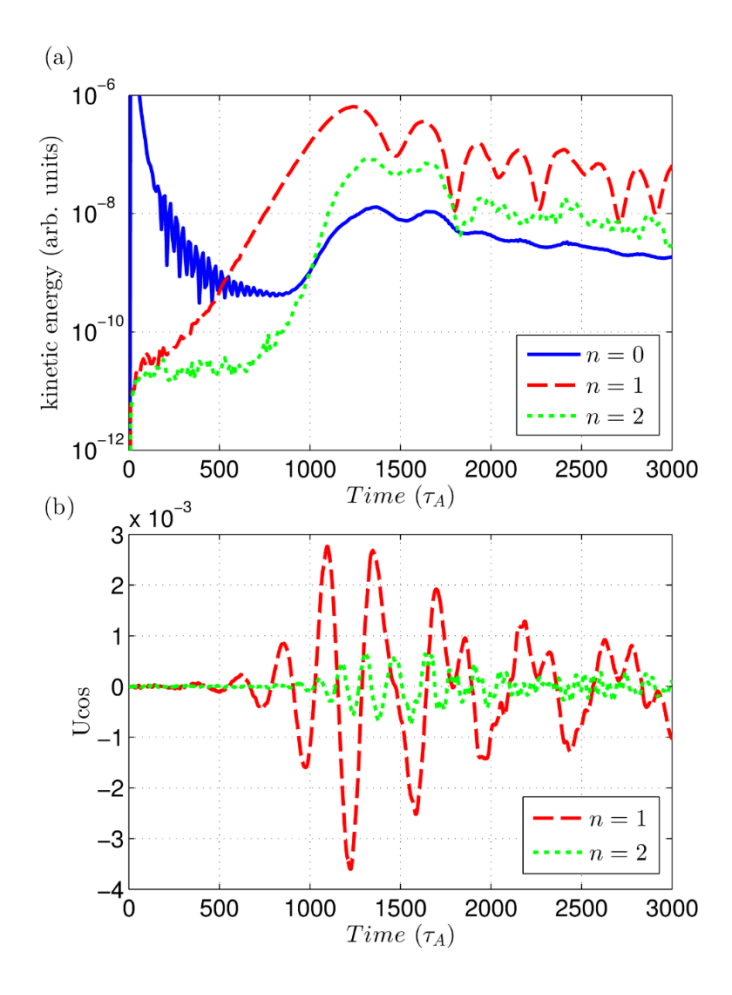


FIG. 5. (a) Kinetic energy evolution from n=0 to n=2, (b) amplitudes of m/n=1/1 and m/n=2/2 fishbones.

The mode structure of the m/n=1/1 and m/n=2/2 fishbones are shown in figures 6 (a) and (b), and the comparisons of the mode structures of the m/n=1/1 and m/n=2/2 fishbones from simulations and experimental measurements are shown in figures 6 (c) and (d), which shows good agreements. In addition, the mode frequencies of the simulated m/n=1/1 and m/n=2/2 fishbones during linear phase are around 12.2 kHz and 24.4 kHz, and the mode frequencies without rotation from experiment are around 14 kHz and 28 kHz. As a result, the simulated mode structures and frequencies of both the m/n=1/1 and m/n=2/2 fishbones are consistent with EAST experimental measurements.

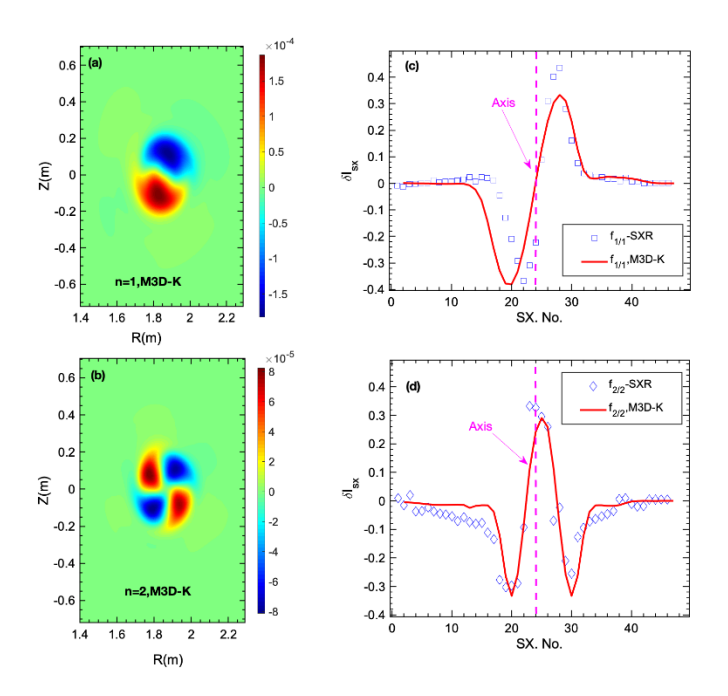
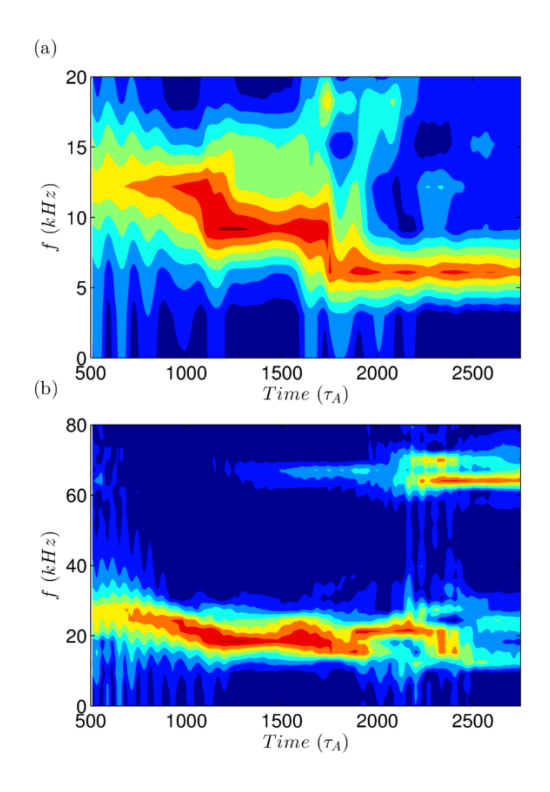


FIG. 6. Mode structures of both the m/n=1/1 and m/n=2/2 fishbones from simulations and experimental measurements.

Mode frequency evolutions of the m/n=1/1 and m/n=2/2 fishbones are shown in figure 7. It is found that the frequency of the m/n=2/2 fishbone is around twice of the m/n=1/1 fishbone, and they chirp down together. At later nonlinear phase, the frequency of the m/n=2/2 fishbone chirps up and it transits to a high frequency mode. The high frequency mode is identified as a BAE because the mode frequency is around $\omega_{n=2}=0.138~\omega_A$ corresponding to 64.0 kHz, which is consistent with the frequency of BAE accumulation point in MHD limit $\omega_{BAE}=\sqrt{\Gamma\beta}\,\omega_A=0.140~\omega_A$, where Γ is the specific heat coefficient. When the rotation frequency is added, the simulated BAE frequency is around 76 kHz, which is also consistent with the experiment observed BAE with frequency in the range of [60 80] kHz.



In general, the wave-particle resonant condition is given by $n\omega_{\phi} - p\omega_{\theta} - \omega = 0$, where ω_{ϕ} is the toroidal transit frequency, ω_{θ} is the poloidal transit frequency, and ω is the mode frequency. Time evolution of beam ion distribution in phase space is shown in figure 8, in which df/f_{θ} denotes the fast ion distribution change df compared to initial fast ion distribution f_{θ} . During the linear phase (at $t = 750 \tau_{A}$ in figure 8 (a)), the large df/f_{θ} structure is consistent with the resonant conditions $\omega_{\phi} = 0.025 \omega_{A}$ for the m/n=1/1 fishbone and $2\omega_{\phi} = 0.050 \omega_{A}$ for the m/n=2/2 fishbone, which means both the fishbones satisfy the same resonant line. During the early nonlinear phase (at $t = 1500 \tau_{A}$ in figure 8 (b)), the frequency of the m/n=2/2 fishbone chirps down together with the m/n=1/1 fishbone, and the beam ions are redistributed in the central region. During the later nonlinear phase (at $t = 2900 \tau_{A}$ in figure 8 (c)) when the BAE is excited, the corresponding resonant line $2\omega_{\phi} + 2\omega_{\theta} - 0.138\omega_{A} = 0$ is located in the redistribution region of beam ions, which shows the excitation of BAE is related to beam ion transport in phase space.

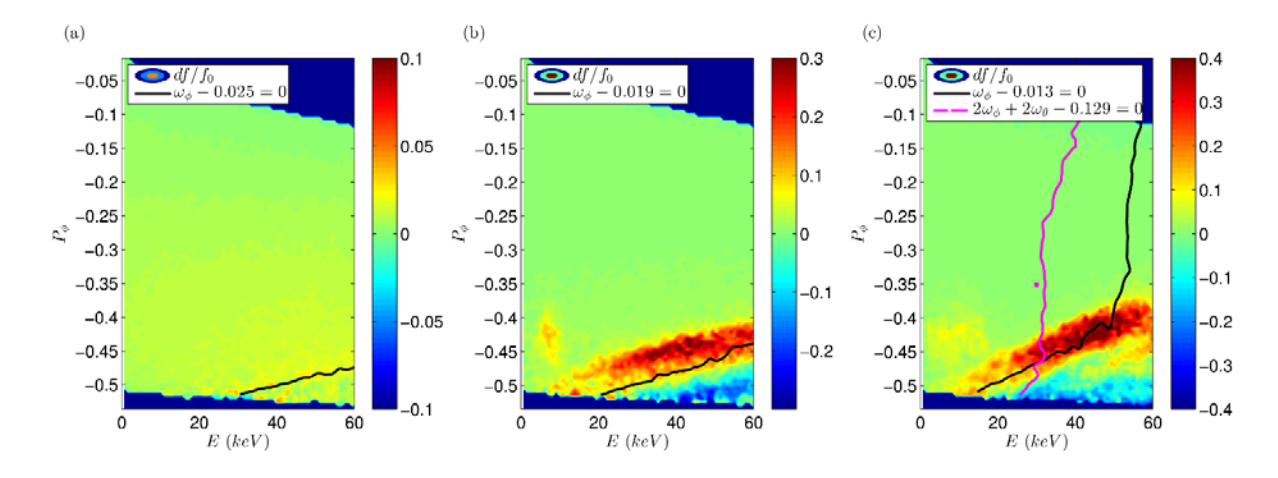


FIG. 8. Distribution change of fast ions df compared to initial fast ion distribution fo in phase space.

4. SUMMARY AND CONCLUSIONS

In conclusion, a systematic investigation of fishbone instabilities with both m/n=1/1, 2/2 mode numbers in EAST with neutral beam injection has been carried out experimentally and numerically.

Experimentally, we employ diagnostics such as SXR to study the details of fishbones. We find that the fishbone mode is characterized by a strong harmonic with mode numbers m/n=2/2. The frequency of the m/n=2/2 fishbone mode is twice that of the m/n=1/1 mode. Neutron flux drops around 7% during fishbones with m/n=1/1 and m/n=2/2 components. Upon reducing the electron density, we observe the disappearance of the m/n=2/2 fishbone mode, followed by the emergence of a high-frequency BAE with an amplitude only one percent of the fishbone mode. There is no clear sawtooth precursor in small sawtooth crash at $t\sim5.3$ s. However, there is a precursor, which is believed driven by thermal plasma, presented before big sawtooth crash at $t\sim5.9$ s. Additionally, a synthetic method is applied to obtain the m=2 fishbone spatial structure using SXR diagnostic with one line-integrated array combined with M3D-K code simulations.

Numerical simulations with the global kinetic-MHD code M3D-K show that the m/n=2/2 high frequency fishbone branch is linearly stable, but nonlinearly grows due to the coupling with the m/n=1/1 low frequency fishbone branch. The frequency of the m/n=2/2 fishbone is 24.4 kHz, which is twice of the m/n=1/1 fishbone frequency with 12.2 kHz. Both the m/n=1/1 and m/n=2/2 fishbone frequencies chirp down together during early nonlinear phase, while BAE is excited at later nonlinear phase of the m/n=2/2 fishbone. Energetic particle nonlinearity is dominant for the m/n=2/2 fishbone saturation and transition to BAE. The mode frequencies and structures of the simulated fishbones, and the simulated BAE frequency are consistent with the experimental measurements.

ACKNOWLEDGEMENTS

This work is supported by National Key R&D Program of China under Grant Nos. 2019YFE03050002 and 2022YFE03010003, the Strategic Priority Research Program of Chinese Academy of Sciences under Grant No. XDB0790202, and the National Natural Science Foundation of China under Grant No. 12275309. The numerical calculations in this paper were performed on the ShenMa High Performance Computing Cluster in Institute of Plasma Physics, Chinese Academy of Sciences.

REFERENCES

- [1] FASOLI A. et al., Nuclear Fusion, Nucl. Fusion 47 2007 S264
- [2] MCGUIRE K. et al., Physics Review Letters, Phys. Rev. Lett. 50 1983 891-5
- [3] CHEN L. et al., Physics Review Letters, Phys. Rev. Lett. 52 1984 1122-5
- [4] COPPI B., PORCELLI F., Physics Review Letters, Phys. Rev. Lett. 57 1986 2272–5
- [5] FU G. Y. et al. Physics of Plasmas, Phys. Plasmas 13 5 (2006) 052517
- [6] PARK W. et al. Physics of Plasmas, Phys. Plasmas 6 5 (1999) 1796